

## Interactions between cleaved (Hg,Cd)Te surfaces and deposited overlayers of Al and In

G. D. Davis, N. E. Byer, R. A. Riedel, and G. Margaritondo

Citation: [Journal of Applied Physics](#) **57**, 1915 (1985); doi: 10.1063/1.335455

View online: <http://dx.doi.org/10.1063/1.335455>

View Table of Contents: <http://scitation.aip.org/content/aip/journal/jap/57/6?ver=pdfcov>

Published by the [AIP Publishing](#)

---

### Articles you may be interested in

[Summary Abstract: Growth of Ge overlayers onto \(HgCd\)Te: A comparison between cleaved and ion-sputtered surfaces](#)

J. Vac. Sci. Technol. A **5**, 1479 (1987); 10.1116/1.574581

[Summary Abstract: Deposition of thin Al and Au overlayers onto sputtered \(HgCd\)Te surfaces](#)

J. Vac. Sci. Technol. A **4**, 850 (1986); 10.1116/1.573792

[Summary Abstract: Deposition of Al overlayers onto cleaved \(HgCd\)Te surfaces](#)

J. Vac. Sci. Technol. A **3**, 981 (1985); 10.1116/1.573370


[Deposition of Au overlayers onto cleaved \(Hg,Cd\)Te surfaces](#)

J. Vac. Sci. Technol. A **2**, 546 (1984); 10.1116/1.572442

[Interaction of thin layers of Al and Ge with cleaved \(Hg,Cd\)Te surfaces](#)

J. Vac. Sci. Technol. A **1**, 1726 (1983); 10.1116/1.572217

---


The Shimadzu logo, consisting of a stylized 'S' inside a circle.**SHIMADZU**  
Excellence in Science

**Powerful, Multi-functional UV-Vis-NIR and FTIR Spectrophotometers**

Providing the utmost in sensitivity, accuracy and resolution for applications in materials characterization and nano research

- Photovoltaics
- Polymers
- Thin films
- Paints
- Ceramics
- DNA film structures
- Coatings
- Packaging materials

[Click here to learn more](#)

A row of four Shimadzu spectrophotometers. From left to right: a small benchtop model, a larger benchtop model with a sample holder, a large floor-standing model with a large sample compartment, and a very large floor-standing model with a large sample compartment and a control panel.

# Interactions between cleaved (Hg, Cd)Te surfaces and deposited overlayers of Al and In

G. D. Davis and N. E. Byer

*Martin Marietta Laboratories, 1450 South Rolling Road, Baltimore, Maryland 21227*

R. A. Riedel and G. Margaritondo

*Department of Physics, University of Wisconsin, Madison, Wisconsin 53706*

(Received 6 September 1984; accepted for publication 8 November 1984)

The interactions between the clean, cleaved  $\text{Hg}_{0.72}\text{Cd}_{0.28}\text{Te}$  surfaces and thin evaporated layers of Al and In have been investigated with ultraviolet photoelectron spectroscopy using synchrotron radiation. Deposition of ultrathin layers of either metal was found to deplete the surface of much of its Hg by breaking the Hg-Te bonds to form a very thin interlayer of  $\text{Al}_2\text{Te}_3$  or one of the several indium tellurides. In contrast, no interaction between the metals and the CdTe component was observed. Upon deposition of additional Al, a metallic Al overlayer was grown, with some Te diffusing to the surface. Some of the Hg freed by the initial reaction diffused into the semiconductor and formed a degenerate  $n^+$  layer capable of ohmically coupling  $n$ -type material to the metallic overlayer.

## I. INTRODUCTION

The compound semiconductor (Hg, Cd)Te is of interest technologically because its narrow but adjustable band gap makes it an excellent material for infrared detectors. From a more basic perspective, it is of interest because it is a pseudobinary semiconductor alloy in which one constituent is only loosely bound.

Many investigations have been reported over the last few years using surface-sensitive techniques to study the passivation of the (Hg, Cd)Te surface<sup>1-17</sup> and, to a lesser extent, the stability of the material.<sup>18-21</sup> However, similar studies of the metallization of the (Hg, Cd)Te surface have just begun,<sup>22-24</sup> despite the successful use of surface-sensitive measurements to understand the interactions between various metals and other semiconductors.<sup>25-28</sup>

Such studies of other semiconductors have indicated that, in most cases, electronic states at or near the interface govern the electron transport between the semiconductor and the metal. For III-V materials, these states are generally thought to be caused by defects in the semiconductor that are induced by the metal through various processes, including chemical reactions, in-diffusion of the contact metal, and out-diffusion of one of the components of the semiconductor.<sup>25-28</sup> These mechanisms, which can involve a decomposition of the semiconductor near the interface, generally dominate interactions between reactive metals and semiconductors such as (Hg, Cd)Te that have low thermodynamic stabilities.

Our previous measurements on metal-(Hg, Cd)Te interfaces supported the expectation.<sup>22-24</sup> Very thin layers of Al reacted strongly with the substrate, resulting in a loss of more than half of the Hg originally present on the surface after deposition of only 1-Å Al. In contrast, deposition of unreactive overlayers (Au or Ge) caused no depletion of Hg. In this paper, we report on more complete experiments involving the deposition of Al overlayers of much greater thicknesses than in our earlier studies<sup>22,23</sup> and In overlayers in which growth of metallic thin films was observed following formation of a reacted interlayer.

## II. EXPERIMENT

The  $p$ -type  $\text{Hg}_{0.72}\text{Cd}_{0.28}\text{Te}$  samples were obtained from Cominco American in the form of elliptical wafers with {111} faces. They were subsequently cut into several strips with <110> axes so that they could be cleaved *in situ* using a knife edge and anvil. Measurements were made using a Perkin-Elmer double-pass cylindrical mirror analyzer (CMA) with preretarding grids and a "grasshopper" monochromator at the Synchrotron Radiation Center of the University of Wisconsin-Madison. Photon energies were generally chosen so that the kinetic energies of the photoelectrons of interest were ~75–80 eV (~45 eV for Al 2p). Spectra were occasionally taken at both higher and lower photon energies to vary the electron mean free path so as to provide information on the depth distribution of the different elements.

The Al and In overlayers were deposited by evaporation from a tungsten basket and their thicknesses were monitored by a quartz oscillator. To avoid high-temperature loss of Hg from exposed surfaces,<sup>21</sup> the (Hg, Cd)Te samples were transferred from an introduction chamber after baking the ultrahigh vacuum (UHV) analysis chamber. Operating pressures were in the low  $10^{-10}$  Torr range. Pressures during deposition ranged from the mid  $10^{-10}$  to low  $10^{-9}$  Torr range for In, and from the low  $10^{-9}$  to low  $10^{-8}$  Torr range for Al. No contamination was detected on the cleaved or metal-covered surfaces reported here. Some oxidation of the Al was seen, however, on surfaces deposited the previous day and on the surface for which the pressure during Al deposition rose to the high  $10^{-8}$  to low  $10^{-7}$  Torr range.

All data are initially displayed in the conventional form of peak intensities normalized to the corresponding value for the clean, cleaved surface. Further analysis of the aluminum results are obtained with the use of surface behavior diagrams (SBD's), a recently developed method of interpreting quantitative surface-sensitive measurements.<sup>4,29,30</sup> These SBD's are similar in appearance to ternary or quaternary phase diagrams in that a surface composition is expressed as a sum of the compositions of three or four basis compounds. They differ, however, in that they display surface composi-

tional information instead of bulk structural information and in that the equilibrium requirement is relaxed so that changes in the surface chemistry can be examined during irreversible reactions,<sup>29-30</sup> sputter-depth profiles,<sup>4</sup> or deposition of overlayers.

To analyze the data by this method, the peak height measurements of the Hg  $5d_{5/2}$ , Cd  $4d_{5/2}$ , and the Te  $4d_{5/2}$  photoelectron lines and the peak area measurements of the Al  $2p$  line were converted into atomic concentrations. Sensitivity factors were developed from the spectra of cleaved surfaces for the semiconductor components. The Al sensitivity factor was obtained by comparing the spectra of our highest Al coverages with that of pure Al; the extra emission was identified as Al in  $\text{Al}_2\text{Te}_3$  and its intensity was compared with that of the Te. Excellent consistency was found from spectrum to spectrum; the greatest uncertainty was associated with Al due to the absence of an intrinsic standard.

The atomic concentrations thus calculated were converted to molar concentrations of HgTe, CdTe,  $\text{Al}_2\text{Te}_3$ , and Al as follows. The Hg and Cd were assigned to HgTe and CdTe, respectively. Any Te in excess of the HgTe and CdTe requirements was assumed to be in the  $\text{Al}_2\text{Te}_3$  form. Similarly, Al in excess of the  $\text{Al}_2\text{Te}_3$  requirements was attributed to metallic Al. Such assignments correlated well with line shape changes of the Al peak.

### III. RESULTS

#### A. Aluminum

Valence band and core level spectra of a cleaved  $\text{Hg}_{0.72}\text{Cd}_{0.28}\text{Te}$  (110) surface before and after several depositions of Al are shown in Fig. 1. Several features of these spectra are worth noting and will be elaborated on in subsequent figures. Most apparent is a decrease in the cation peak heights with a more rapid attenuation of the Hg  $5d$  peak and a persistence of the Te signal. These trends are shown more clearly in Fig. 2. During the early stages of deposition, the Cd signal falls as expected from overlayer attenuation considerations assuming a mean free path in Al of  $1.9 \text{ \AA}$ .<sup>31</sup> (The decrease at the very initial stages may be less than expected,

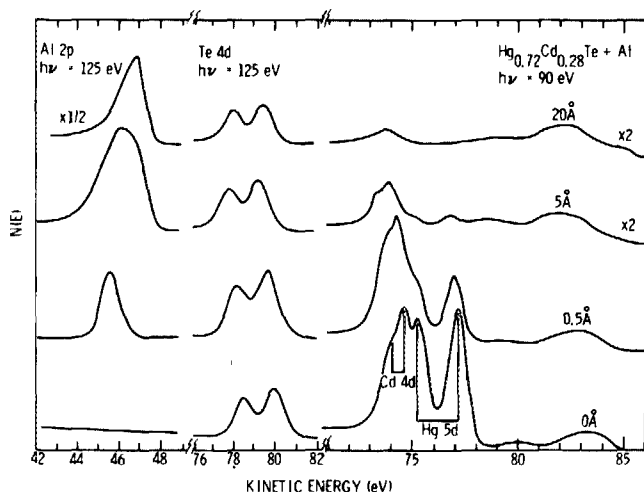


FIG. 1. UPS spectra of  $\text{Hg}_{0.72}\text{Cd}_{0.28}\text{Te}$ : a freshly cleaved surface ( $0 \text{ \AA}$ ) and surfaces after deposition of  $0.5$ -,  $5$ -, and  $20$ - $\text{\AA}$  Al. ( $1$ - $\text{\AA}$  Al  $\sim 6 \times 10^{14}$  atoms/ $\text{cm}^2$ ).

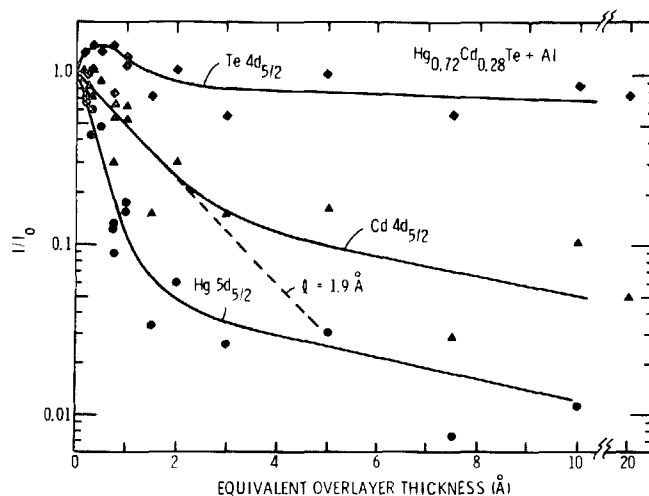


FIG. 2. Normalized core-level intensities of  $\text{Hg}_{0.72}\text{Cd}_{0.28}\text{Te}$  as a function of Al coverage. The dashed line shows the intensity predicted from an abrupt interface and an uniform overlayer with an electron mean free path of  $1.9 \text{ \AA}$ .<sup>31</sup>

as discussed below.) In contrast, as reported earlier,<sup>22,23</sup> the Hg signal falls much more rapidly, indicating a loss of Hg from the surface. At higher coverages, the peak heights for both cations continue to decrease, but at a slower rate than expected from the inelastic scattering of the photoelectrons through a uniformly thick overlayer. The behavior of the Te signal, on the other hand, is quite different. Initially, the peak height rises by  $\sim 50\%$  at  $0.5$ - $\text{\AA}$  Al coverage before beginning a very slow decline so that the signal persists with little attenuation even after deposition of  $20$ - $\text{\AA}$  Al.

During the growth of the Al overlayers, the core levels of each element present move upward in binding energy (downward in kinetic energy) as shown in Fig. 3. The semiconductor components exhibit a shift of  $0.4$ – $0.8 \text{ eV}$  upon the deposition of the first  $1$ – $2$ - $\text{\AA}$  Al, with the kinetic energies of the cation peaks remaining constant following deposition of more Al. In contrast, with the higher coverages, the Te signal reverses the direction of the shift so that at  $20 \text{ \AA}$ ,  $0.3$ – $0.4 \text{ eV}$  of the shift at  $2 \text{ \AA}$  has been recovered. During the initial stage, the Te peak broadens as reflected by the increase in the ratio of the valley height between the two Te  $4d$  components to the  $4d_{5/2}$  peak height. This broadening is likely to be a reflection of two chemical states of Te that are not resolvable. The reason for the reversal of energy shift with higher coverage is not known; no broadening is seen during this stage to indicate a third, more tightly bound, chemical state.

A similar, but more dramatic, behavior is seen for the Al  $2p$  peak. This peak initially shifts downward in kinetic energy, but after  $1$ - $\text{\AA}$  Al coverage, it shows a dramatic upward shift of  $\sim 1.5 \text{ eV}$  to higher kinetic energy (Fig. 4). At very low coverages, only one peak, representing chemically bound Al (probably  $\text{Al}_2\text{Te}_3$ ) is seen, and it exhibits the same trend as peaks of Hg and Cd. Beginning with  $\sim 2 \text{ \AA}$  of coverage, however, the Al peak broadens as a second component, representing elemental Al, appears. This component then continues to grow until it dominates the peak at the higher coverages. However, the higher-binding-energy component continues to be present even at the highest coverages, as can

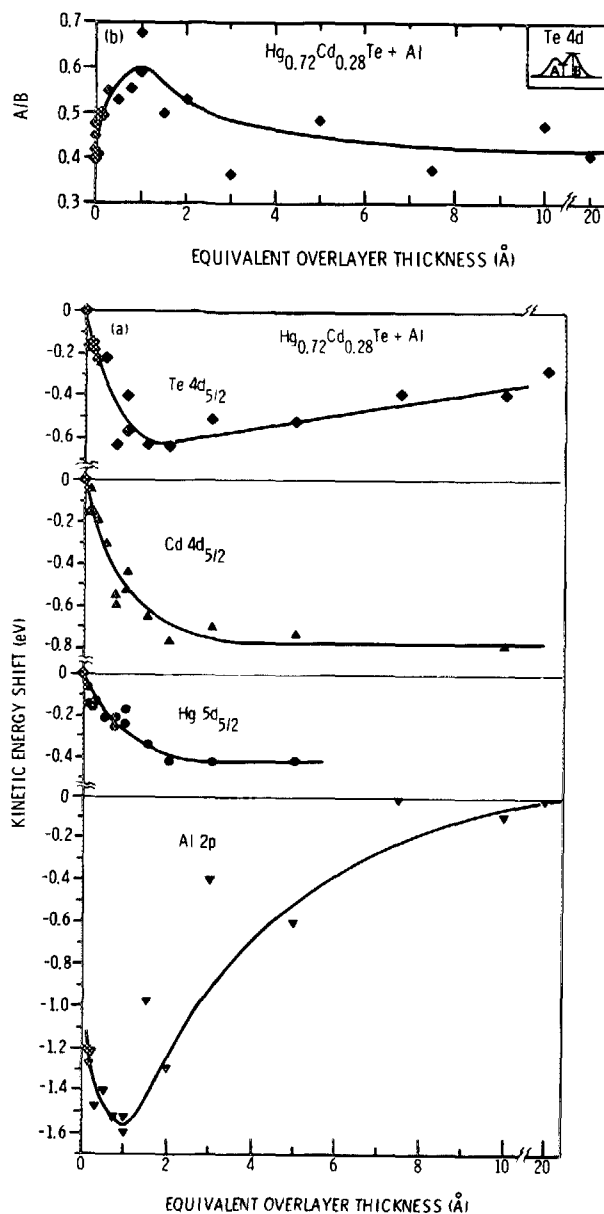


FIG. 3. (a) Kinetic energy shifts of the Te 4d<sub>5/2</sub>, Cd 4d<sub>5/2</sub>, Hg 5d<sub>5/2</sub>, and Al 2p photoelectrons as a function of Al coverage. For the semiconductor components, the zero energy is given by the spectrum from a clean surface; for Al the zero energy is given by the spectrum for the highest Al coverage. (b) Broadness of the Te 4d peak, given by the ratio of the quantities defined in the insert, as a function of Al coverage.

be seen by comparing these measurements with that of a very thick Al overlayer on copper.<sup>32</sup>

At two coverages, 5- and 20-Å Al, the Te peak was measured at three different photon energies (and, hence, three different electron mean free paths) in order to provide an indication of the Te distribution with depth. The results, normalized to spectra of the cleaved surface, are given in Table I. Results for a 5-Å Al overlayer indicate a subsurface Te-rich volume—probably the same Te-rich surface seen after deposition of subangstrom amounts of Al (Fig. 2). For 20-Å Al coverage, the trend is reversed—more Te is seen at the surface. Apparently the initial Te-rich region is too deep to contribute to the signal, while Te has diffused through the overlayer to segregate at the surface.

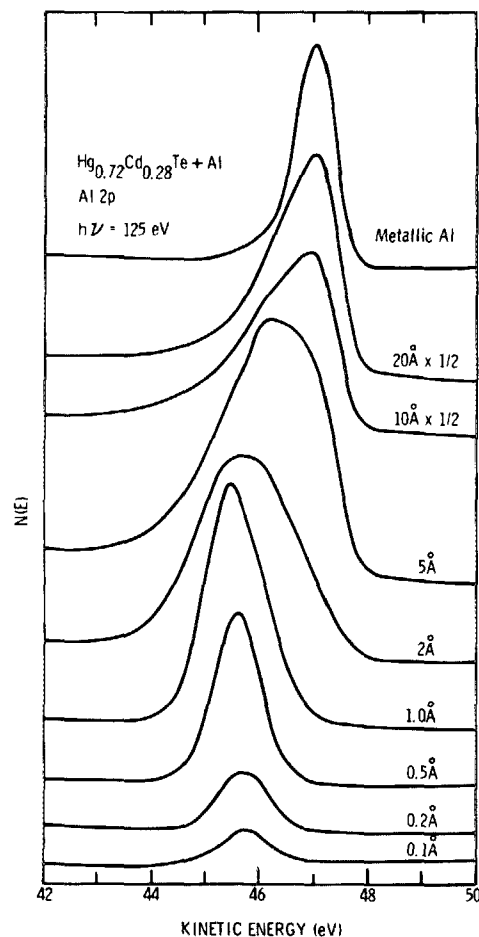


FIG. 4. Al 2p line shape as a function of Al coverage. Also shown is a completely metallic Al peak (taken at  $h\nu = 135$  eV and shifted 10 eV).<sup>32</sup>

The behavior of the surface upon Al deposition is further elucidated by presenting the data in the form of a HgTe-CdTe-Al<sub>2</sub>Te<sub>3</sub>-Al SBD (Fig. 5). Initially, the surface composition evolves in the HgTe-CdTe-Al<sub>2</sub>Te<sub>3</sub> plane along a constant CdTe-concentration line indicating a replacement of the HgTe with Al<sub>2</sub>Te<sub>3</sub> without significantly masking the CdTe. (The increase in the Te signal, then, reflects the greater fraction of Te in Al<sub>2</sub>Te<sub>3</sub> than in HgTe.) Once growth of metallic Al begins (and the surface composition leaves the HgTe-CdTe-Al<sub>2</sub>Te<sub>3</sub> plane), the HgTe and CdTe are both rapidly attenuated. However, instead of proceeding directly toward the Al vertex, the surface composition traces a C-shaped path reflecting the outdiffusion of Te (in the form of Al<sub>2</sub>Te<sub>3</sub>) which is diminished as the Al overlayer grows.

TABLE I. Te 4d<sub>5/2</sub> peak heights for 5- and 20-Å Al (normalized to a cleaved surface) as a function of kinetic energy.

Al coverage (Å)	Photoelectron kinetic energy (eV)			
	50	55	80	104
5	0.80	...	0.52	0.60
20	...	0.79	0.90	1.1
Surface sensitivity →				

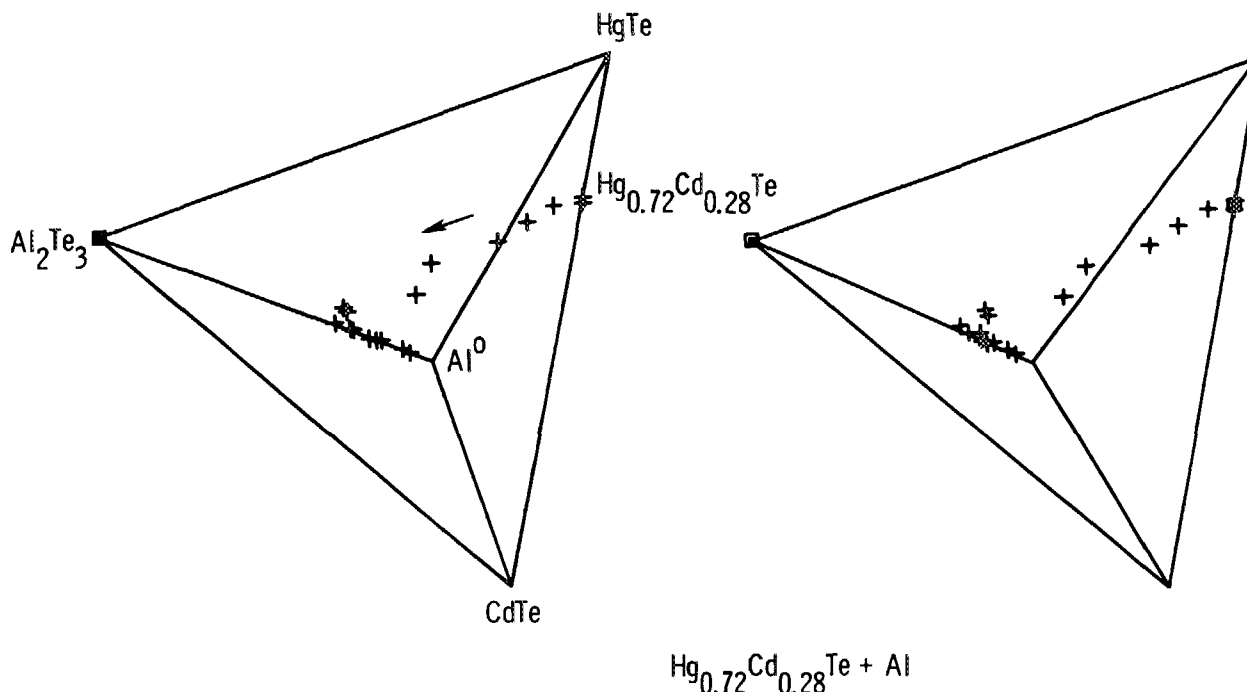


FIG. 5. HgTe-CdTe-Al<sub>2</sub>Te<sub>3</sub>-Al surface behavior diagram showing the evolution of the surface composition upon Al deposition. The surface composition traces a C-shaped path beginning on the HgTe-CdTe axis and ending near the Al vertex. (The two views of the SBD are rotated by 7°. Examination with a stereo viewer will provide a three-dimensional image.)

## B. Indium

The behavior of the (Hg,Cd)Te surface upon deposition of In is, in many respects, very similar to that upon deposition of Al. Figures 6 and 7 show representative spectra of In-covered surfaces and the normalized intensities of the semiconductor components, respectively. Again, we see an initial decrease in the Cd signal close to that expected from mean-free-path considerations (assuming  $l \sim 4 \text{ \AA}^{33}$ ) while the Hg peak height falls off much more quickly. (At higher coverages, the attenuation is slower than predicted.) The surface depletion of Hg, relative to Cd, is essentially completed when 1 Å of metal is deposited, and is the same for Al and In (Fig. 8).

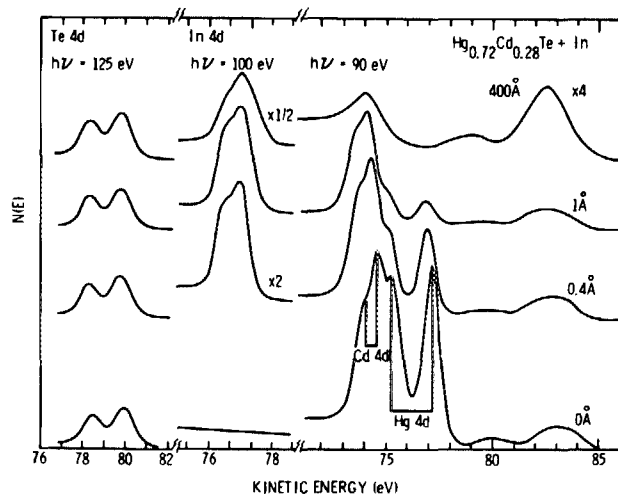


FIG. 6. UPS spectra of Hg<sub>0.72</sub>Cd<sub>0.28</sub>Te: a freshly cleaved surface and surfaces after deposition of 0.4–1-, and 400-Å In. (1-Å In  $\sim 4 \times 10^{14}$  atoms/cm<sup>2</sup>).

The Te signal increases following In deposition as it does after Al deposition. For all In coverages, however, the Te signal remains higher than the value for the cleaved surface, in contrast to the behavior noted with evaporation of Al.

Upon growth of the In overlayer, the photoelectron peaks of the semiconductor components all shift upward in binding energy (downward in kinetic energy) by  $\sim 0.2$ – $0.6$  eV (0.1–0.2 eV less than that observed for Al) (Fig. 9). For Hg and Te, this shift is quickly completed so that little additional shift is seen after  $\sim 0.5$ -Å In. Energy movement of the In peak is small, consistent with the more limited range of binding energy shifts seen in In compounds compared to those of Al compounds.<sup>34,35</sup> Nonetheless, there is some indication of an initial downward shift followed by an upward shift in kinetic energy, possibly indicating the growth of metallic In on top of an In-Te complex.

## IV. DISCUSSION

The behavior of the Hg<sub>0.72</sub>Cd<sub>0.28</sub>Te surface upon deposition of these metals can be explained by the low stability of HgTe. During the initial steps of Al and In deposition, the chemisorbed metal breaks the weak Hg-Te bonds with the concomitant formation of Al<sub>2</sub>Te<sub>3</sub> or one of the several indium tellurides: In<sub>2</sub>Te, InTe, In<sub>3</sub>Te<sub>4</sub>, In<sub>2</sub>Te<sub>3</sub>, and In<sub>2</sub>Te<sub>5</sub>.<sup>36</sup> The Cd-Te bonds, on the other hand, appear unaffected as a sharp CdTe/Al interface is maintained, as illustrated by initial evolutionary path in the SBD of Fig. 5, and the absence of freed Cd. Such behavior is qualitatively consistent with thermodynamic predictions; Table II shows that HgTe is the least stable of any of the pertinent tellurides.<sup>36,37</sup> Consequently, the interfacial heats of reaction  $\Delta H_R$  for reactions such as

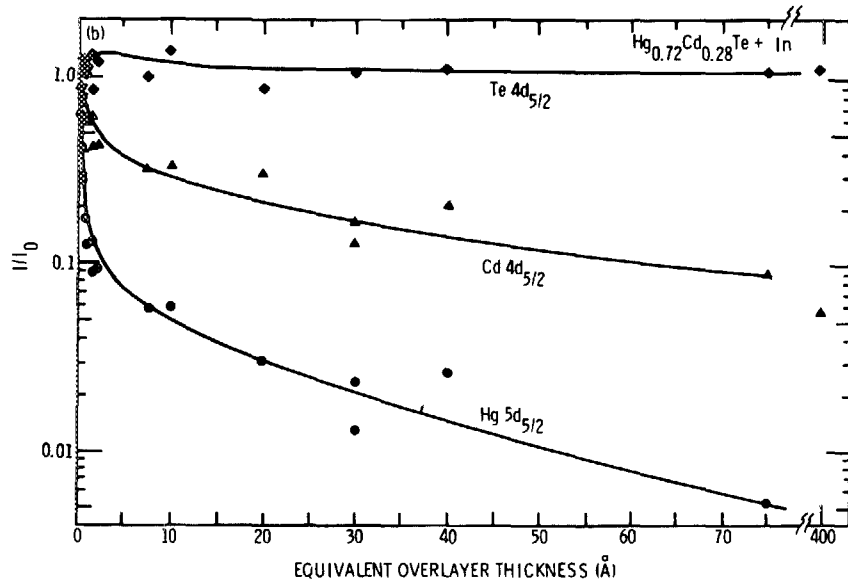
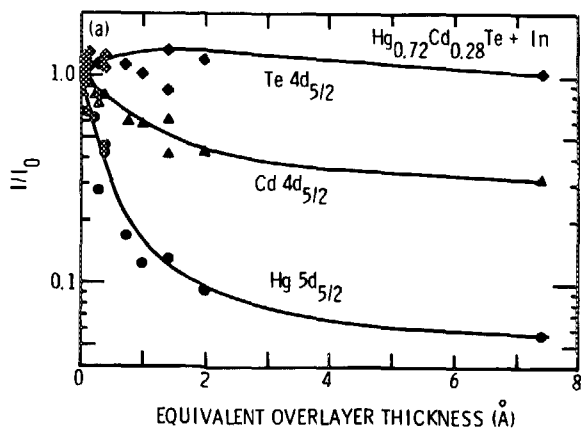


FIG. 7. Normalized core-level intensities of  $\text{Hg}_{0.72}\text{Cd}_{0.28}\text{Te}$  as a function of In coverage: (a) low coverages and (b) higher coverages.

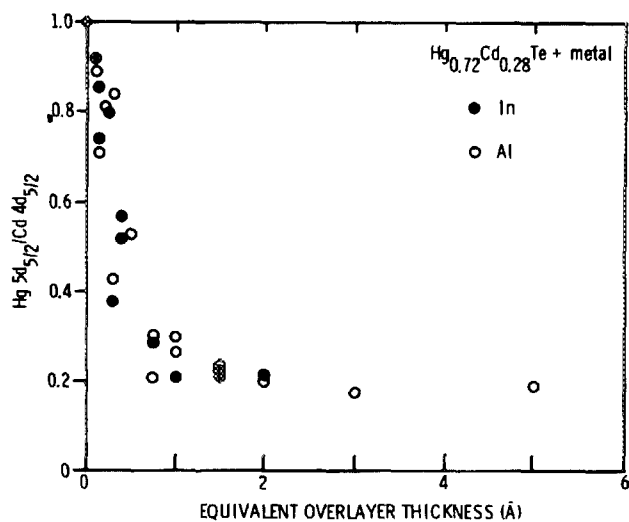


FIG. 8. Ratio of  $\text{Hg } 5d_{5/2}$  and  $\text{Cd } 4d_{5/2}$  peak heights, normalized to the cleaved surface, as a function of metal coverage.

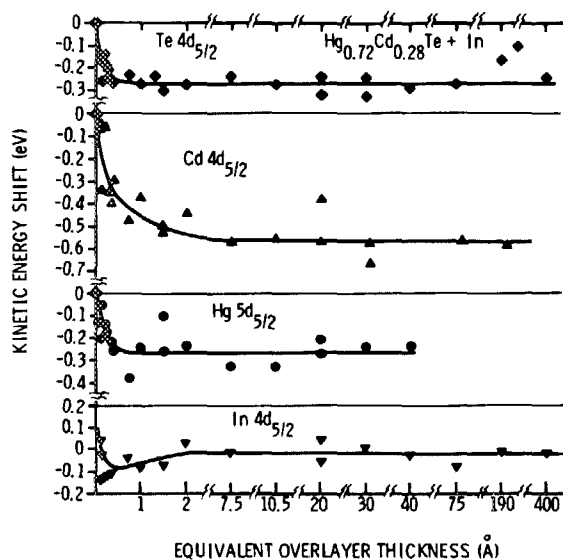


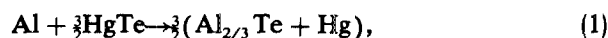
FIG. 9. Kinetic energy shifts of the  $\text{Te } 4d_{5/2}$ ,  $\text{Cd } 4d_{5/2}$ ,  $\text{Hg } 5d_{5/2}$ , and  $\text{In } 4d_{5/2}$  photoelectrons as a function of In coverage. For the semiconductor components, the zero energy is given by the spectrum from a clean surface; for In, the zero energy is given by the spectrum for the highest In coverage.

TABLE II. Heats of formation of selected tellurides and interfacial heats of reaction for Al and In on (Hg, Cd)Te.

Compound	$\Delta H_R$ (kcal/mole)					
	$\Delta H_f$ (kcal/mole Te)		HgTe		CdTe	
	a	b	a	b	a	b
HgTe	7.6	-10.0	...	...	...	...
CdTe	-24.1	-22.1	...	...	...	...
Al <sub>2</sub> Te <sub>3</sub>	-25.4	-26.0	-26.7	-24.0	-1.95	-5.85
In <sub>2</sub> Te	-19.05		-5.7		2.5	
InTe	-17.2	-23.0	-9.6	-13.0	6.9	0.90
In <sub>3</sub> Te <sub>4</sub>	-15.8		-10.9		11.1	
In <sub>2</sub> Te <sub>3</sub>	-15.3	-15.8	-11.6	-8.7	13.2	9.4
In <sub>7</sub> Te <sub>5</sub>	-9.2		-4.0		37.2	

\* Reference 33.

\* Reference 34.



defined as

$$\Delta H_R = \frac{2}{3}[H_F(\text{HgTe}) - H_F(\text{Al}_{2/3}\text{Te})], \quad (2)$$

indicate the formation of an interfacial reaction product.<sup>25-27</sup> The stability of the CdTe is slightly surprising since the  $\Delta H_R$  of Al<sub>2</sub>Te<sub>3</sub> and several of the indium tellurides with respect to CdTe (Table II) is less than the critical  $\Delta H_R$  of  $\sim 11$  kcal/mol for the reaction to occur,<sup>25-27</sup> and since freed Cd has been detected following deposition of Al (but not In) onto CdTe.<sup>38</sup> The discrepancy between the prediction that In would react with CdTe [as a homogeneous material or in the (Hg, Cd)Te alloy] and the apparent lack of the reaction could reflect uncertainty in the heats of formation of these compounds as demonstrated by the differences in values reported by Mills<sup>36</sup> and Wagman *et al.*<sup>37</sup> On the other hand, the differences in behavior when Al (and possibly In) is deposited on CdTe in the pure material or in the alloy are likely to be a result of the increased strength of Cd-Te bonds in the alloy.<sup>14,19,20</sup> A decrease in the reactivity of the Cd-Te bond in (Hg, Cd)Te relative to that in CdTe has been reported recently for the oxidation of (Hg, Cd)Te<sup>14</sup>; the oxidation rate of the alloy corresponded to that of the HgTe mole fraction with no apparent contribution from the CdTe portion.

The spatial extent of the reacted layer on the alloy is quite small as reflected by (1) the quick and abrupt bend upward of the SBD evolutionary path toward the metallic Al vertex (Fig. 5), (2) the growth of the elemental Al peak after deposition of only  $\sim 1$  Å (Fig. 4), (3) the rise and fall of the Te signal by  $\sim 1$  Å of Al (Fig. 2), and (4) the stabilization of the Hg/Cd ratio (Fig. 8). Such coverage ( $\sim 6 \times 10^{14}$  atoms/cm<sup>2</sup>) corresponds to approximately one Al atom for each (Hg, Cd)Te molecule on the surface. Once the surface becomes stabilized with respect to Al, metallic Al grows on top of the reacted layer.

During the initial stages of Al deposition, the kinetic energies of all the peaks decrease by up to  $\sim 0.8$  eV (i.e., the binding energies increase). These shifts denote a movement of the Fermi level from an inverted position at the top of band gap<sup>22,23,39</sup> to a degenerate position inside the conduction band. This shift is likely to be caused by some of the freed Hg diffusing into the semiconductor where excess ca-

tions act as donors.<sup>25</sup> The ease at which (Hg, Cd)Te can become degenerate is due to the low density of states (DOS) at and near the CBM, only  $\sim 1\%$  of the valence-band DOS.<sup>40,41</sup> The low DOS, in turn, makes the photoemission signal from these states not visible in our measurements. This initial movement of the Fermi level is solely responsible for the energy shifts of the Cd and bound Al peaks; the shifts of the Hg and Te peaks, on the other hand, also reflect changes in the chemical state. The Hg becomes less bound with respect to Cd by 0.3–0.4 eV, indicating residual freed Hg, possibly weakly bound to the lattice, that was not lost from the surface. Concomitantly, the Te peak broadens slightly (Fig. 3) representing the detection of Te in both (Hg, Cd)Te and Al<sub>2</sub>Te<sub>3</sub>; the substrate component is rapidly attenuated, however, the peak returns to its original width.

The Al spectra also show Al<sub>2</sub>Te<sub>3</sub>. At first this is the only component visible; as the metallic peak grows, the bound component persists in the form of a high binding energy shoulder as the Te outdiffuses (Figs. 4 and 5). This outdiffused Te appears to segregate at the Al surface as suggested by the greater peak intensity (relative to those of the cleaved surface) at kinetic energies corresponding to lower mean free paths (Table I).

The cation signals also persist at the higher coverages with intensities low, but higher than expected. This may be caused by clustering of the Al, as suggested by the early appearance of the metallic Al peak, the lack of dissociated Cd to outdiffuse, and the constant Hg/Cd ratio.

A similar series of events appears to occur during In deposition even though some of the effects, such as the chemical shifts of the In peak, are less pronounced: the chemisorbed In breaks the Hg-Te bonds, but not the Cd-Te bonds, and forms an indium telluride. Some of the freed Hg diffuses into the bulk to make the inverted surface region degenerate, some remains less bound on the surface, and any remainder is lost to the vacuum. The In starts to cluster at lower coverages than in the case of Al (Figs. 7 and 9), and this also allows the cation to be detected at high coverages without indication of dissociated Cd to outdiffuse. Te, on the other hand, does outdiffuse so that the Te signal is as high for the heaviest coverages of In as it is for the cleaved surface, suggesting that the indium telluride formed is one of the tellurium-rich compounds.

These results explain why In and Al can be used to form ohmic contacts to  $n$ -type (Hg, Cd)Te. Mercury freed during the interfacial reactions dope the surface region to form an  $n^+$  region which couples the metal to the semiconductor. By the same argument, however, In and Al would not be suitable as contacts to  $p$ -type material.

## V. SUMMARY

We have shown that the deposition of Al or In onto clean, cleaved  $\text{Hg}_{0.72}\text{Cd}_{0.28}\text{Te}$  surfaces results in a breaking of the Hg-Te bonds, but not the Cd-Te bonds, of the surface and the formation of a thin reacted layer of aluminum or indium telluride. With subsequent deposition, a metallic overlayer is grown with Te outdiffusing to the surface. Some of the freed Hg diffuses into the near surface region to form a degenerate  $n^+$  layers—explaining the effectiveness of these materials for forming ohmic contacts to  $n$ -type material.

## ACKNOWLEDGMENTS

We gratefully acknowledge the valuable technical assistance of A. C. Goldberg and the useful discussions with W. A. Beck. We are also grateful to Ed Rowe and to the entire staff of the University of Wisconsin Synchrotron Radiation Center (supported by NSF Grant No. DMR83-13523) for their expert assistance. This work was funded in part by ONR under Grant No. N00014-80-C-0908.

- <sup>1</sup>T. S. Sun, S. P. Buchner, and N. E. Byer, *J. Vac. Sci. Technol.* **17**, 1067 (1980).
- <sup>2</sup>G. D. Davis, T. S. Sun, S. P. Buchner, and N. E. Byer, *J. Vac. Sci. Technol.* **19**, 472 (1981).
- <sup>3</sup>J. S. Ahearn, G. D. Davis, and N. E. Byer, *J. Vac. Sci. Technol.* **20**, 756 (1982).
- <sup>4</sup>G. D. Davis, S. P. Buchner, W. A. Beck, and N. E. Byer, *Appl. Surf. Sci.* **15**, 238 (1983).
- <sup>5</sup>U. Solzbach and H. J. Richter, *Surf. Sci.* **97**, 191 (1980).
- <sup>6</sup>M. Seelmann-Eggebert, G. Brandt, and H. J. Richter, *J. Vac. Sci. Technol. A* **2**, 11 (1984).
- <sup>7</sup>O. Ganschow, H. M. Nitz, L. Wiedmann, and A. Benninghoven in *Secondary Ion Mass Spectrometry—SIMS II*, edited by A. Benninghoven, C. A. Evans, Jr., R. A. Powell, R. Shimizu, and H. A. Storms, Springer Series in Chemical Physics, Vol. 19 (Springer, Berlin, 1979), p. 275.
- <sup>8</sup>U. Kaiser, O. Ganschow, L. Wiedmann, and A. Benninghoven, *J. Vac. Sci. Technol. A* **1**, 657 (1983).
- <sup>9</sup>D. R. Rhiger and R. E. Kvaas, *J. Vac. Sci. Technol.* **21**, 168 (1982).
- <sup>10</sup>D. R. Rhiger and R. E. Kvaas, *J. Vac. Sci. Technol.* **21**, 448 (1982).

- <sup>11</sup>P. Morgen, J. A. Silberman, I. Lindau, W. E. Spicer, and J. A. Wilson, *J. Electr. Mater.* **11**, 597 (1982).
- <sup>12</sup>P. Morgen, J. Silberman, I. Lindau, W. E. Spicer, and J. A. Wilson, *J. Vac. Sci. Technol.* **21**, 161 (1983).
- <sup>13</sup>J. A. Silberman, D. Laser, I. Lindau, and W. E. Spicer, *J. Vac. Sci. Technol. A* **1**, 1706 (1983).
- <sup>14</sup>J. A. Silberman, D. Laser, I. Lindau, W. E. Spicer, and J. A. Wilson, *J. Vac. Sci. Technol. B* **2**, 589 (1984).
- <sup>15</sup>S. P. Kowalczyk and J. T. Cheung, *J. Vac. Sci. Technol.* **18**, 944 (1981).
- <sup>16</sup>Y. Nemirovsky, R. Goshen, and I. Kidron, *J. Appl. Phys.* **53**, 4888 (1982).
- <sup>17</sup>A. B. Christie, I. Sutherland, and J. M. Walls, *Surf. Sci.* **135**, 225 (1983).
- <sup>18</sup>W. A. Harrison, *J. Vac. Sci. Technol. A* **1**, 1672 (1983).
- <sup>19</sup>W. E. Spicer, J. A. Silberman, P. Morgen, I. Lindau, J. A. Wilson, A.-B. Chen, and A. Sher, *Physica* **117B/118B**, 60 (1983).
- <sup>20</sup>W. E. Spicer, J. A. Silberman, I. Lindau, A.-B. Chen, A. Sher, and J. A. Wilson, *J. Vac. Sci. Technol. A* **1**, 1735 (1983).
- <sup>21</sup>H. M. Nitz, O. Ganschow, U. Kaiser, L. Wiedmann, and A. Benninghoven, *Surf. Sci.* **104**, 365 (1981).
- <sup>22</sup>R. R. Daniels, G. Margaritondo, G. D. Davis, and N. E. Byer, *Appl. Phys. Lett.* **42**, 50 (1983).
- <sup>23</sup>G. D. Davis, N. E. Byer, R. R. Daniels, and G. Margaritondo, *J. Vac. Sci. Technol. A* **1**, 1726 (1983).
- <sup>24</sup>G. D. Davis, W. A. Beck, N. E. Byer, R. R. Daniels, and G. Margaritondo, *J. Vac. Sci. Technol. A* **2**, 546 (1984).
- <sup>25</sup>L. J. Brillson, *Surf. Sci. Rept.* **2**, 123 (1982), and the references therein.
- <sup>26</sup>L. J. Brillson, C. F. Brucker, A. D. Katnani, N. G. Stoffel, R. Daniels, and G. Margaritondo, *Surf. Sci.* **132**, 212 (1983).
- <sup>27</sup>L. J. Brillson, *J. Phys. Chem. Solids* **44**, 703 (1983).
- <sup>28</sup>W. E. Spicer, P. W. Chye, P. R. Skeath, C. Y. Su, and I. Lindau, *J. Vac. Sci. Technol.* **16**, 1422 (1979).
- <sup>29</sup>G. D. Davis, T. S. Sun, J. S. Ahearn, and J. D. Venables, *J. Mater. Sci.* **17**, 1807 (1982).
- <sup>30</sup>G. D. Davis, J. S. Ahearn, and J. D. Venables, *J. Vac. Sci. Technol. A* **2**, 763 (1984).
- <sup>31</sup>C. J. Powell, R. J. Steiner, P. B. Needham, and T. J. Driscoll, *Phys. Rev. B* **16**, 1370 (1977).
- <sup>32</sup>R. R. Daniels (unpublished work).
- <sup>33</sup>I. Lindau and W. E. Spicer, *J. Electron Spectrosc. Relat. Phenom.* **3**, 409 (1974).
- <sup>34</sup>T. A. Carlson, *Photoelectron and Auger Spectroscopy* (Plenum, New York, 1975), pp. 355, 365.
- <sup>35</sup>C. D. Wagner, W. M. Riggs, L. E. Davis, J. F. Moulder, and G. E. Muilenberg, *Handbook of X-Ray Photoelectron Spectroscopy* (Perkin Elmer, Eden Prairie, MN, 1979), pp. 50, 116.
- <sup>36</sup>K. C. Mills, *Thermodynamic Data for Inorganic Sulphides, Selenides, and Tellurides* (Butterworths, London, 1974), pp. 30, 32, 42.
- <sup>37</sup>D. D. Wagman, W. H. Evans, V. B. Parker, I. Halow, S. M. Bailey, and R. H. Schumm, *Selected Values of Chemical Thermodynamic Properties* (NBS Technical Note 270, Washington, 1968), Vol. 3, pp. 212, 225, 254; Vol. 4, p. 5.
- <sup>38</sup>M. H. Patterson and R. H. Williams, *J. Cryst. Growth* **59**, 281 (1982).
- <sup>39</sup>J. A. Silberman, P. Morgen, I. Lindau, W. E. Spicer, and J. A. Wilson, *J. Vac. Sci. Technol.* **21**, 154 (1982).
- <sup>40</sup>E. Finkman and Y. Nemirovsky, *J. Appl. Phys.* **53**, 1052 (1982).
- <sup>41</sup>R. Dornhaus and G. Nimtz, *Solid State Physics: Springer Tracts in Modern Physics* **78**, edited by G. Hohler (Springer, Berlin, 1976), p. 1.